Weighted tensorized fractional Brownian textures

Céline ESSER[1] Claire LAUNAY[2] Laurent LOOSVELDT[1] Béatrice VEDEL[2]

[1]Département de Mathématique, Université de Liège, Belgique

[2]UMR CNRS 6205, LMBA, Université de Bretagne Sud, Vannes, France

Résumé – Nous présentons un nouveau modèle de textures obtenues comme réalisations de champs appelés champs browniens fractionnaires pondérément tensorisés. Ils sont obtenus par une relaxation de la structure de produit tensoriel qui apparaît dans la définition des draps browniens fractionnaires. Des propriétés statistiques de ces champs, telles que l'auto-similarité, la stationnarité des accroissements rectangulaires, sont obtenues. Une généralisation à des champs à auto-similarité matricielle est proposée et des simulations basées sur la représentation spectrale sont effectuées.

Abstract – We present a new model of textures, obtained as realizations of a new class of fractional Brownian fields. These fields, called *weighted tensorized fractional Brownian fields*, are obtained by a relaxation of the tensor-product structure that appears in the definition of fractional Brownian sheets. Statistical properties such as self-similarity and stationarity of rectangular increments are obtained. An operator scaling extension is defined and we provide simulations of the fields using their spectral representation.

1 Introduction

The modeling of natural phenomena, in particular textures, by random objects has led to the introduction of numerous stochastic processes and fields. The most famous and historically first example is the well-known Brownian motion, which was extended to fractional Brownian motions by Kolmogorov in his seminal paper of 1940 [10], to define "Gaussian spirals" in Hilbert spaces. Given a Hurst parameter $H \in (0,1)$, the fractional Brownian motion B^H is the unique Gaussian process with stationary increments satisfying the self-similarity relation $B^H_{at} \overset{(d)}{=} a^H B_t$ for any $a, t > 0$, where $\overset{(d)}{=}$ means that the equality holds in the sense of finite-dimensional distributions. It can be characterized via its harmonizable representation:

$$\forall t \in \mathbb{R}_+,\ B^H_t = \int_{\mathbb{R}} \frac{e^{it\xi} - 1}{|\xi|^{H+1/2}} d\hat{\mathbf{W}}(\xi), \tag{1}$$

Several extensions have been proposed in higher dimensions. In particular, two natural generalizations have been introduced. The first one is the Levy fractional Brownian motion (LFBM) of Hurst index $H \in (0,1)$, also called fractional Brownian field (see e.g. [13]). It is the unique real-valued isotropic Gaussian field Y^H with stationary increments satisfying the self-similarity property $Y^H_{a\mathbf{x}} \overset{(d)}{=} a^H Y^H_{\mathbf{x}}$, where "isotropic" means that the field is invariant in law by rotation. Again, it can be defined using its harmonizable representation:

$$Y^H_{\mathbf{x}} = \int_{\mathbb{R}^N} \frac{e^{i\langle \mathbf{x}, \boldsymbol{\xi}\rangle} - 1}{\|\boldsymbol{\xi}\|^{H+\frac{N}{2}}} d\hat{\mathbf{W}}(\boldsymbol{\xi}) \tag{2}$$

where $\langle \cdot, \cdot \rangle$ denotes the standard scalar product in $\mathbb{R}^N$.

A second famous extension is given by the fractional Brownian sheet (fBs) studied in [2, 9]. For a given vector $\mathbf{H} = (H_1, ...H_N) \in (0,1)^N$, the fBs of Hurst index $\mathbf{H}$ is a real-valued centered Gaussian random field $S^{\mathbf{H}}$ with the following harmonizable representation

$$S^{\mathbf{H}}_{\mathbf{x}} = \int_{\mathbb{R}^N} \prod_{m=1}^{N} \frac{e^{ix_m\xi_m} - 1}{|\xi_m|^{H_m+\frac{1}{2}}} d\hat{\mathbf{W}}(\boldsymbol{\xi}). \tag{3}$$

Setting $H_m = \frac{1}{2}$ for each $m \in \{1, \dots, N\}$ yields the standard Brownian sheet. While LFBMs are isotropic, fBs exhibit a strong "tensor-product" structure even when $H_m = H$ for all $m \in \{1, \dots, N\}$ and no longer have stationary increments but instead possess rectangular stationary increments (see Definition 3.2). Nevertheless, this field has been widely studied for its interesting mathematical aspects, including fractal dimensions [3], geometric features, local times, and many more.

Further developments. Focusing on the class of Gaussian fields, the two previously mentioned extensions of the fractional Brownian motions can be seen as particular cases of more general models. Important properties have been introduced in these models, such as anisotropy with different properties along directions.

The Operator Scaling Gaussian Random Fields (OSGRF) introduced in [6] satisfy a self-similarity condition

$$\forall a > 0, \quad Z_{a^E\mathbf{x}} \overset{(d)}{=} a^H Z_{\mathbf{x}}$$

for some $H > 0$, where E is a $N \times N$ matrix with eigenvalues having positive real parts, and where $a^E = \sum_{k\geq 0} \frac{\ln(a)^k E^k}{k!}$. These fields have been shown to exhibit anisotropic regularity properties [4], which offer strategies for numerical estimations of the parameters of the model [12].

Goals, contribution and outline. The strong effect of the tensor-product in Brownian sheets make them insufficiently realistic for modeling many textures. However, in urban data or medical images, some textures may exhibit a reticulated structure. The contribution of the paper is to provide new Gaussian textures with a controlled tensor-product effect. This effect emerges as a parameter α goes from 1 to 0, yielding the fractional Brownian sheet for $\alpha = 0$ and a field closer to an LFBM in terms of regularity for $\alpha = 1$. Note that the regularity of the fields has been studied in detail in [8], where associated "weighted tensorized" function spaces have also been defined. This notion of weighted tensorized regularity naturally arises in partial differential equations such as the electronic Schrödinger equation [16]. In this paper, we focus on statistical properties

of self-similarity, stationarity and variance of increments. We provide an extension to the anisotropic cases and simulations of these fields.

2 Definition of the fields

Let $\alpha \in [0,1]$ and $H \in (0,1)$, we set

$$H_\alpha^+ := (1+\alpha)H \text{ and } H_\alpha^- := (1-\alpha)H$$

and we define a weighted tensorized fractional Brownian field (WTFBF) as the Gaussian field $\{X^{\alpha,H}_{(x_1,x_2)}\}_{(x_1,x_2)\in\mathbb{R}^2}$ given by

$$X^{\alpha,H}_{(x_1,x_2)} := \int_{\mathbb{R}^2} \frac{(e^{ix_1\xi_1}-1)(e^{ix_2\xi_2}-1)}{\phi_{\alpha,H}(\xi_1,\xi_2)} d\hat{\mathbf{W}}(\boldsymbol{\xi}) \quad (4)$$

where the function

$$\phi_{\alpha,H}(\xi_1,\xi_2) = \min(|\xi_1|,|\xi_2|)^{H_\alpha^- + \frac{1}{2}} \max(|\xi_1|,|\xi_2|)^{H_\alpha^+ + \frac{1}{2}}$$

denotes the square root of the inverse of the spectral density of the field. In the sequel, we also use the notation

$$\mathcal{K}^{\alpha,H}_{(x_1,x_2)}(\xi_1,\xi_2) := \frac{(e^{ix_1\xi_1}-1)(e^{ix_2\xi_2}-1)}{\phi_{\alpha,H}(\xi_1,\xi_2)}$$

for the kernel in the stochastic integral (4). The formula mimics the definition of the fractional Brownian sheet and carefully provides homogeneity properties for the function $\phi_{\alpha,H}$ which are crucial to define self-similar fields. However, the parameter α introduces a diversity of the spectral law leading to non-classical regularity of the fields. Note that the field (4) is well-defined since this last kernel belongs to $L^2(\mathbb{R}^2)$. Note furthermore that the Fourier transform of $\mathcal{K}^{\alpha,H}_{(x_1,x_2)}$ is real. Indeed, one has

$$\begin{aligned}&\Im\left(e^{-i(t_1\xi_1+t_2\xi_2)}(e^{ix_1\xi_1}-1)(e^{ix_2\xi_2}-1)\right)\\ &=\sin((x_1-t_1)\xi_1+(x_2-t_2)\xi_2)-\sin(-t_1\xi_1+(x_2-t_2)\xi_2)\\ &\quad-\sin((x_1-t_1)\xi_1-t_2\xi_2)+\sin(-t_1\xi_1-t_2\xi_2)\end{aligned}$$

which is an odd function in (ξ_1,ξ_2). It follows that

$$\int_{\mathbb{R}^2} \frac{\Im\left(e^{-i(t_1\xi_1+t_2\xi_2)}(e^{ix_1\xi_1}-1)(e^{ix_2\xi_2}-1)\right)}{\phi_{\alpha,H}(\xi_1,\xi_2)} d\boldsymbol{\xi} = 0.$$

It implies that $\widehat{\mathcal{K}^{\alpha,H}_{(x_1,x_2)}}$ is real, hence so is the field $X^{\alpha,H}_{(x_1,x_2)}$.

3 Basic properties

Proposition 3.1. *For all $\alpha \in [0,1]$ and $H \in (0,1)$, the process $X^{\alpha,H}$ is self-similar: for all $a > 0$, $\{X^{\alpha,H}_{(ax_1,ax_2)}\}_{(x_1,x_2)\in\mathbb{R}^2} \overset{(d)}{=} \{a^{2H}X^{\alpha,H}_{(x_1,x_2)}\}_{(x_1,x_2)\in\mathbb{R}^2}$.*

Proof. The self-similarity property obviously comes from the homogeneity of the function $\phi_{\alpha,H}$. □

These fields offer new examples of self-similar fields with stationary rectangular increments, complementing the examples presented in [2, 11] and allowing simulations of them. Note that the class of Gaussian self-similar processes with stationary increments is reduced to fractional Brownian processes. Extensions to 2D are provided by the class of OSGRF but the property of rectangular stationary increments seems to allow more richness in terms of regularity.

Definition 3.2. *If $\{X_{(x_1,x_2)}\}_{(x_1,x_2)\in\mathbb{R}^2}$ is a field and if $(x_1,x_2),(y_1,y_2) \in \mathbb{R}^2$, we set*

$$\begin{aligned}&\Delta X_{(x_1,x_2);(y_1,y_2)}\\ &:= X_{(x_1+y_1,x_2+y_2)} - X_{(y_1,x_2+y_2)} - X_{(x_1+y_1,y_2)} + X_{(y_1,y_2)}.\end{aligned}$$

We say that $\{X_{(x_1,x_2)}\}_{(x_1,x_2)\in\mathbb{R}^2}$ has stationary rectangular increments if, for any $(y_1,y_2)\in\mathbb{R}^2$, we have

$$\{\Delta X_{(x_1,x_2);(y_1,y_2)}\}_{(x_1,x_2)\in\mathbb{R}^2} \overset{(d)}{=} \{X_{(x_1,x_2)}\}_{(x_1,x_2)\in\mathbb{R}^2}.$$

Proposition 3.3. *For all $\alpha \in [0,1]$ and $H \in (0,1)$, the field $\{X^{\alpha,H}_{(x_1,x_2)}\}_{(x_1,x_2)\in\mathbb{R}^2}$ has stationary rectangular increments.*

Proof. It suffices to show that, for any $(y_1,y_2) \in \mathbb{R}^2$, the finite dimensional distributions of $\{X^{\alpha,H}_{(x_1,x_2)}\}_{(x_1,x_2)\in\mathbb{R}^2}$ and $\{\Delta X_{(x_1,x_2);(y_1,y_2)}\}_{(x_1,x_2)\in\mathbb{R}^2}$ have the same characteristic function. First, we remark that for any $(x_1,x_2)\in\mathbb{R}^2$, we get from (4)

$$\Delta X^{\alpha,H}_{(x_1,x_2);(y_1,y_2)} = \int_{\mathbb{R}^2} e^{i(y_1\xi_1+y_2\xi_2)} \mathcal{K}^{\alpha,H}_{(x_1,x_2)}(\xi_1,\xi_2) d\hat{\mathbf{W}}(\boldsymbol{\xi}).$$

Thus, recalling [13, Corollary 6.3.2], we have

$$\begin{aligned}&\mathbb{E}\left(\exp\left(i\sum_{j=1}^n t^{(j)} \Delta X^{\alpha,H}_{(x_1^{(j)},x_2^{(j)});(y_1,y_2)}\right)\right)\\ &= \exp\left(-c_0\int_{\mathbb{R}^2}\left|\sum_{j=1}^n t^{(j)} e^{i(y_1\xi_1+y_2\xi_2)} \mathcal{K}^{\alpha,H}_{(x_1^{(j)},x_2^{(j)})}(\xi_1,\xi_2)\right|^2 d\boldsymbol{\xi}\right)\\ &= \mathbb{E}\left(\exp\left(i\sum_{j=1}^n t^{(j)} X^{\alpha,H}_{(x_1^{(j)},x_2^{(j)})}\right)\right),\end{aligned}$$

for any $(x_1^{(1)},x_2^{(1)}),\dots,(x_1^{(n)},x_2^{(n)}),(y_1,y_2)\in\mathbb{R}^2$ and any $t^{(1)},\dots,t^{(n)}\in\mathbb{R}$, with $c_0 := \frac{1}{2\pi}\int_0^\pi \cos(\theta)^2\, d\theta$. The conclusion follows directly. □

4 Variance of rectangular increments

Estimating the variance of the increments is a classical strategy to derive results on the regularity of sample paths, using a Kolmogorov-type theorem.

Proposition 4.1. *For all $\alpha \in [0,1]$ and $H \in (0,1)$, there is a constant $c_1 > 0$ such that the rectangular increments of $\{X^{\alpha,H}_{(x_1,x_2)}\}_{(x_1,x_2)\in\mathbb{R}^2}$ satisfy*

$$\begin{aligned}&\mathbb{E}(|\Delta X^{\alpha,H}_{(h_1,h_2);(x_1,x_2)}|^2)\\ &\quad\le c_1\left(\max\{|h_1|,|h_2|\}^{1-\alpha}\min\{|h_1|,|h_2|\}^{1+\alpha}\right)^{2H}\end{aligned}$$

for all $(x_1,x_2),(h_1,h_2)\in\mathbb{R}^2$.

Proof. The isometry property of the stochastic integral gives

$$\begin{aligned}&\mathbb{E}\big(|\Delta X^{\alpha,H}_{(h_1,h_2);(x_1,x_2)}|^2\big)\\ &= \int_{\mathbb{R}^2} \frac{|e^{i(x_1+h_1)\xi_1}-e^{ix_1\xi_1}|^2|e^{i(x_2+h_2)\xi_2}-e^{ix_2\xi_2}|^2}{(\phi_{\alpha,H}(\xi_1,\xi_2))^2} d\boldsymbol{\xi}\\ &= \frac{1}{|h_1|\,|h_2|}\int_{\mathbb{R}^2} \frac{|e^{i\eta_1}-1|^2|e^{i\eta_2}-1|^2}{(\phi_{\alpha,H}(\frac{\eta_1}{h_1},\frac{\eta_2}{h_2}))^2} d\boldsymbol{\eta}\end{aligned}$$

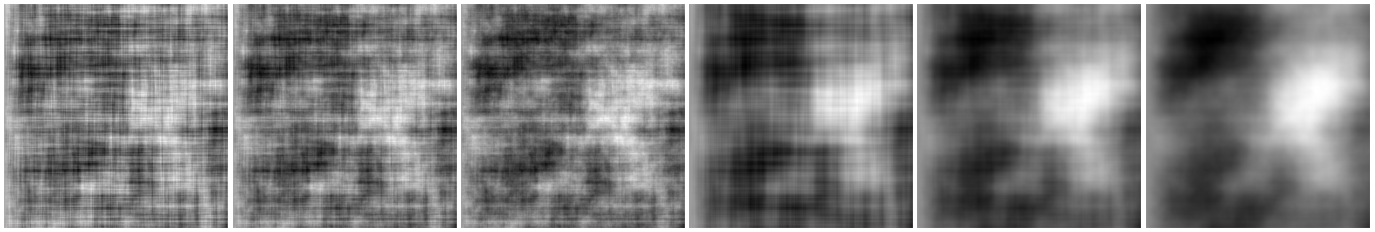

(a) $\alpha = 0$ (b) $\alpha = 0.5$ (c) $\alpha = 1$ (d) $\alpha = 0$ (e) $\alpha = 0.5$ (f) $\alpha = 1$

Figure 1 – Weighted tensorized fractional Brownian fields simulated using a spectral representation approximation method, with parameters (a-c) $H = 0.3$ or (d-f) $H = 0.7$ and (a,d) $\alpha = 0$, (b,e) $\alpha = 0.5$ or (c,f) $\alpha = 1$.

using the change of variables $(\eta_1, \eta_2) = (h_1\xi_1, h_2\xi_2)$. Notice now that if $|h_1| \geq |h_2|$, one has

$$(\phi_{\alpha,H}(\tfrac{\eta_1}{h_1}, \tfrac{\eta_2}{h_2}))^2 \geq \frac{\min(|\eta_1|, |\eta_2|)^{2H_\alpha^- + 1} |\eta_2|^{2H_\alpha^+ + 1}}{|h_1|^{(2H_\alpha^- + 1)} |h_2|^{(2H_\alpha^+ + 1)}}.$$

It implies $\mathbb{E}\big(|\Delta X^{\alpha,H}_{(h_1,h_2);(x_1,x_2)}|^2\big) \leq c_1 |h_1|^{2H_\alpha^-} |h_2|^{2H_\alpha^+}$ with

$$c_1 = \int_{\mathbb{R}^2} \frac{|e^{i\eta_1} - 1|^2 |e^{i\eta_2} - 1|^2}{\min(|\eta_1|, |\eta_2|)^{2H_\alpha^- + 1} |\eta_2|^{2H_\alpha^+ + 1}} d\boldsymbol{\eta} \qquad (5)$$

if $|h_1| \geq |h_2|$. The same argument for $|h_1| < |h_2|$ leads to the conclusion. □

Regarding the rectangular increments, a generalization of Kolmogorov's continuity theorem allows us to assert that there exists a modification of the field $\{X^{\alpha,H}_{(x_1,x_2)}\}_{(x_1,x_2)\in\mathbb{R}^2}$ which is nearly *locally* (H_α^+, H_α^-)*-rectangular Hölder*. This means that for every bounded intervals I, J of $\mathbb{R}$, every $x_1 \in I$, $x_2 \in J$ and every $\varepsilon > 0$, there exists a positive finite random variable $C > 0$ such that almost surely

$$\begin{aligned} &|\Delta X^{\alpha,H}_{(h_1,h_2);(x_1,x_2)}| \\ &\leq C \left(\max\{|h_1|, |h_2|\}^{(1-\alpha)} \min\{|h_1|, |h_2|\}^{(1+\alpha)} \right)^{H-\varepsilon} \end{aligned}$$

for all $h_1, h_2 \in \mathbb{R}$ such that $x_1 + h_1 \in I$ and $x_2 + h_2 \in J$, see [8] for details.

5 Anisotropic extension

The model introduced in the previous sections can be extended to provide anisotropic textures by imposing an operator scaling property.

We consider $\beta_1, \beta_2 \in (0, 2)$ such that $\beta_1 + \beta_2 = 2$, and set

$$X^{\alpha,H,\beta_1,\beta_2}_{(x_1,x_2)} := \int_{\mathbb{R}^2} \frac{(e^{ix_1\xi_1} - 1)(e^{ix_2\xi_2} - 1)}{\phi_{\alpha,H,\beta_1,\beta_2}(\xi_1, \xi_2)} d\hat{\mathbf{W}}(\boldsymbol{\xi}) \qquad (6)$$

where $\phi_{\alpha,H,\beta_1,\beta_2}(\xi_1, \xi_2) = \phi_{\alpha,H}\big(|\xi_1|^{\frac{1}{\beta_1}}, |\xi_2|^{\frac{1}{\beta_2}}\big)$. If $\max(\beta_1, \beta_2) - 1 < 2H < 3\min(\beta_1, \beta_2) - 1$, the corresponding field is well-defined and satisfies

$$X^{\alpha,H,\beta_1,\beta_2}_{a^D\mathbf{x}} \overset{(d)}{=} a^{2H} X^{\alpha,H,\beta_1,\beta_2}_{\mathbf{x}} \qquad (7)$$

with $D = \mathrm{diag}(\beta_1, \beta_2)$ and $a^D\mathbf{x} = (a^{\beta_1}x_1, a^{\beta_2}x_2)$. These fields then satisfy anisotropic properties of regularities that will be explored in a forthcoming work. Extensions to non-diagonal operators could also be investigated.

6 Simulation

Several strategies have been developed to simulate Gaussian random fields. Methods based on an explicit expression for the covariance of the field allow for exact simulations that preserve statistical properties such as stationarity (see [5]).When the covariance is not explicitly known but is known along radial directions, the turning-bands method can be employed, as in [7] to simulate some anisotropic fields. Using the spectral density of the field, approximations of AFBF have been obtained in [1]. Given that we only have an integral expression of the covariance, we adopt this approach to generate a WTFBF. This spectral representation method involves discretizing the field in the Fourier domain [14]. Although its main limitations include challenges in assessing the convergence of the approximation, as well as the potential for the inverse Fourier transform to disrupt the statistical properties of the field, this method is still widely used to generate stationary and non-stationary Gaussian random fields. In the case of stationary random fields, Shinozuka and Deodatis [14] proved that the generated samples verify ergodic properties, in the sense that the spatial mean and autocorrelation function of any sample converge to the theoretical mean and autocorrelation function of the field, as the sample size increases. It is also fast and easy to perform as it involves fast Fourier transforms. Approximations based on wavelet methods could be used, but they are known to be quite slow in practice even if they provide the best approximation rate by a series in the case of FBF.

The results presented in Figures 1 and 2 are generated using a spectral representation approximation on a discrete grid of size $(M + 1) \times (M + 1)$, with $M = 512$. For a given WTFBF $\{X^{\alpha,H}_{(x_1,x_2)}\}_{(x_1,x_2)\in\mathbb{R}^2}$, the strategy involves generating W, a collection of independent standard complex Gaussian variables of size $(2M \times 2M)$. These variables are then multiplied by a function g. Next, in both directions successively, a 1D Fourier transform is applied, followed by subtracting the value of the field at the origin. If we set $g(x, y) = (\phi_{\alpha,H}(x, y))^{-1}\mathbf{1}_{\{x\neq 0, y\neq 0\}}$ for $(x, y) \in \mathbb{R}^2$, the generated field $x^{\alpha,H}$ is given, for all $k_1, k_2 \in \{0, \ldots, M\}$, by

$$x^{\alpha,H}\left(\tfrac{k_1}{M}, \tfrac{k_2}{M}\right) = \mathcal{R}\left(y_2\left(\tfrac{k_1}{M}, \tfrac{k_2}{M}\right) - y_2\left(0, \tfrac{k_2}{M}\right)\right),$$

where for any $n_1 \in \{-M + 1, \ldots, M\}$

$$y_1\left(n_1, \tfrac{k_2}{M}\right) = \sum_{n_2=-M+1}^{M} W(n_1, n_2) g(\pi n_1, \pi n_2)\, e^{-\frac{2i\pi n_2 k_2}{2M}},$$

$$y_2\left(\tfrac{k_1}{M}, \tfrac{k_2}{M}\right) = \pi \sum_{n_1=-M+1}^{M} \left(y_1\left(n_1, \tfrac{k_2}{M}\right) - y_1(n_1, 0)\right) e^{-\frac{2i\pi n_1 k_1}{2M}}.$$

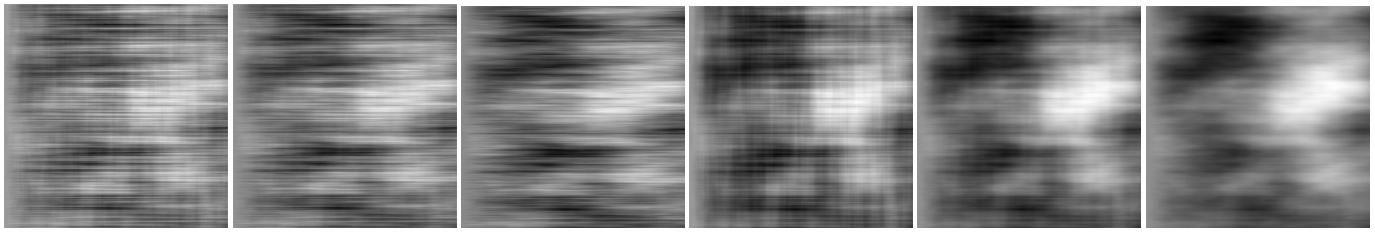

(a) $\alpha = 0$ (b) $\alpha = 0.5$ (c) $\alpha = 1$ (d) $\alpha = 0$ (e) $\alpha = 0.5$ (f) $\alpha = 1$

Figure 2 – Anisotropic weighted tensorized fractional Brownian fields simulated using a spectral representation approximation method, with parameters (a-c) $H = 0.4$, $\beta_1 = 0.7$, $\beta_2 = 1.3$ and $\alpha = 0$, $\alpha = 0.5$ or $\alpha = 1$, and (d-f) $H = 0.6$, $\beta_1 = 0.85$, $\beta_2 = 1.15$ and $\alpha = 0$, $\alpha = 0.5$ or $\alpha = 1$.

The same method is used to simulate the anisotropic extension. Figure 1 presents synthesized WTFBFs with various parameters H and α. When $\alpha = 0$, the procedure samples a fBs while, when $\alpha = 1$, the generated texture tends to loose the reticulated aspect and to approach a fractional Brownian field. Figure 2 shows anisotropic WTFBFs. These fields $X^{\alpha,H,\beta_1,\beta_2}$ produce anisotropic textures, where the highest β determines the dominant direction. The images (a-f) illustrate the effects of the parameters α, β and H on the fields. We generated 100 textures of size 512×512, with parameters $H = 0.3$ and $\alpha = 0.5$ to evaluate the statistical properties of the realizations, similarly as in [15]. The results are presented in Table 1. Note that the fields given by the rectangular increments tend to have a mean and a skewness approaching the mean and skewness of the original field and the theoretical mean and skewness, supposed to be zero. Regarding the self-similarity property, the estimated mean and skewness of the rescaled generated textures are close to their theoretical target, zero. In both cases however, the variance seems to be biased. A matlab implementation to generate these textures and reproduce our results is available online (https://github.com/claunay/wtfbf).

Table 1 – Estimated moments of WTFBFs generated by the spectral representation method

	$X^{\alpha,H}$	$\Delta X^{\alpha,H}$	$\frac{1}{a^{2H}} X^{\alpha,H}$
Mean	-2×10^{-4}	-1×10^{-5}	2×10^{-2}
Variance	7.3	10.7	1.4
Skewness	-6×10^{-4}	1×10^{-6}	-0.3

Conclusion

In this paper, we introduced a new model of textures that relaxes the tensor-product structure of fractional Brownian sheets, in an attempt to construct a bridge between fBs and fractional Brownian fields. These textures can appear in medical or urban images and are associated with regularity properties involved partial differential equations. We have shown that these random fields are self-similar and have stationary rectangular increments, with bounded variance. Some simulations illustrate the behavior of these textures for various parameters.

Acknowledgment This work was conducted within the ANR Mistic project (ANR-19-CE40-005).

References

[1] A. Ayache, A. Bonami, and A. Estrade. Identification and series decomposition of anisotropic gaussian fields. *More Progresses In Analysis*, pages 441–450, 2009.

[2] A. Ayache, S. Léger, and M. Pontier. Drap Brownien Fractionnaire. *Pot. Anal.*, 17:31–43, 2002.

[3] A. Ayache and Y. Xiao. Asymptotic properties and Hausdorff dimensions of fractional Brownian sheets. *J. Fourier Anal. Appl.*, 11(4):407–439, 2005.

[4] H. Biermé and C. Lacaux. Hölder regularity for operator scaling stable random fields. *Stoc. Proc. Appl.*, 119(7):2222–2248, 2009.

[5] H. Biermé and C. Lacaux. Fast and exact synthesis of some operator scaling random fields. *Appl. and Comp. Harm. Anal.*, 48(1):293–320, 2020.

[6] H. Biermé, M. Meerschaert, and H.P. Scheffler. Operator Scaling Stable Random Fields. *Stoch. Proc. Appl.*, 117(3):312–332, 2007.

[7] H. Biermé, L. Moisan, and F. Richard. A turning band method for the simulation of anisotropic fractional brownian fields. *J. Comput. Graph. Statist*, 24(3), 2015.

[8] C. Esser, L. Loosveldt, and B. Vedel. Regularity of Weighted Fractional Brownian Fields and associated function spaces. 2024.

[9] A. Kamont. On the fractional anisotropic Wiener field. *Prob. Math. Stat.*, 16(1):85–98, 1996.

[10] A. N. Kolmogorov. Wienersche Spiralen und einige andere interessante Kurven im Hilbertschen Raum. *C. R. (Doklady) Acad. Sci. URSS (N.S.)*, 26:115–118, 1940.

[11] V. Makogin and Y. Mishura. Gaussian multi-self-similar random fields with distinct stationary properties of their rectangular increments. *Sto. Mod.*, 35(4):391–428, 2019.

[12] S.G. Roux, M. Clausel, B. Vedel, S. Jaffard, and P. Abry. Self -similar anisotropic texture analysis : the hyperbolic wavelet transform contribution. *Transaction on Image Processing*, 22(11):4353–4363, 2013.

[13] G. Samorodnitsky and M. S. Taqqu. *Stable non-Gaussian random processes*. Chapman and Hall, New York, 1994.

[14] M. Shinozuka and G. Deodatis. Simulation of multi-dimensional gaussian stochastic fields by spectral representation. *App. Mech. Reviews*, 49(1):29–53, 1996.

[15] L. Vandanapu and M. D. Shields. 3^{rd}-order spectral representation method: Simulation of multi-dimensional random fields and ergodic multi-variate random processes with fft implementation. *Prob. Eng. Mech.*, 64:103–128, 2021.

[16] H. Yserentant. On the regularity of the electronic Schrödinger equation in Hilbert spaces of mixed derivatives. *Numer. Math.*, 98(4):731–759, 2004.